Engineering Structures 75 (2014) 39–50

Contents lists available at ScienceDirect

Engineering Structures

journal homepage: www.elsevier.com/locate/engstruct

Design process for prototype concrete shells using a hybrid cable-net and fabric formwork

Diederik Veenendaal *, Philippe Block

BLOCK Research Group, Institute of Technology in Architecture, ETH Zurich, Stefano-Franscini-Platz 5, 8093, Switzerland

ARTICLE INFO

Article history:
Received 3 November 2013
Revised 20 May 2014
Accepted 21 May 2014

Keywords:
Shell structure
Cable net
Fabric formwork
Flexible formwork
Form finding
Shape optimization

ABSTRACT

This paper sets out to explore the potential of combining a cable net with a fabric, in particular to scale the concept of flexible formworks to the size of large-span roofs and bridges, especially when applying a thin coat of concrete or mortar to form a shell structure. By carefully designing the cable net and its topology, and calculating and controlling the prestressing forces, it is possible to form a wide range of anticlastic shapes, beyond those of the hyperbolic paraboloid.

A complete workflow for the computational design of a shell shape and its corresponding flexible formwork are presented as a proof-of-concept for future work. Two prototype shell structures were built based on this workflow to validate the overall approach, to compare the built geometry with that of the design model and to identify further challenges when developing and scaling up the concept. In addition, a comprehensive overview of flexible formworks for anticlastic shells is presented to frame the present research.

1. Introduction

Concrete shell structures, if properly designed and constructed, are able to cover large spaces at minimal material cost through efficient membrane action.

However, they are challenging to construct, traditionally requiring full and generally rigid formworks, which are both material- and labor-intensive. The materials are often used only once, since they are customized for a specific doubly curved geometry. Due to the amount of work involved, these structures are generally not competitive in a contemporary building environment where labor is expensive.

It is possible to reduce the amount of material, especially of the falsework, by introducing a flexible formwork. In this case, the shuttering is replaced by a fabric, and the falsework by a cable net, supported by an external frame at its boundaries. The challenge is then to design the flexible formwork such that the resulting shape matches the designed geometry.

After summarizing the wider context and the specific objectives of this research project, Section 2 presents a review of historical and recent construction methods for anticlastic (negatively doubly curved) shell structures with an emphasis on flexible formworks. This review is intended to illustrate some of the differences between the combined cable-net and fabric formwork discussed here and flexible formworks in precedent work. In addition, it is used to frame some of the design choices made for two built prototypes. Section 3 presents a complete workflow for the design, optimization and form finding of these cable-net and fabric-formed, anticlastic shell prototypes, before discussing their actual construction in Section 4.

1.1. Context of research project

The workflow and prototype structures, presented in this paper, are intended to further inform and develop the design of the HiLo roof. HiLo is a research and innovation unit for NEST demonstrating ultra-lightweight construction. It is planned as a 16 m × 9 m duplex penthouse apartment for visiting faculty of Empa and Eawag. NEST is a flagship project of Empa and Eawag in collaboration with the ETH Domain. It is a dynamic, modular research and demonstration platform for advanced and innovative building technologies on the Empa–Eawag campus in Dübendorf, Switzerland, to be completed in 2015 (Fig. 1). As a "future living and working lab", NEST consists of a central backbone and a basic grid to accommodate exchangeable living and office modules, such as HiLo, allowing novel materials and components, and innovative systems to be tested, demonstrated and optimized under real-world conditions. HiLo is a collaborative effort of the BLOCK Research Group and the Assistant Professorship of Architecture

* Corresponding author.
E-mail addresses: dveenend@ethz.ch (D. Veenendaal), pblock@ethz.ch (P. Block).

http://dx.doi.org/10.1016/j.engstruct.2014.05.036
0141-0296/

Fig. 1. Visualization of the preliminary design for NEST, with HiLo constructed at the top corner. ©EMPA and Gramazio & Kohler.

and Sustainable Technologies (SuAT), both at the Institute of Technology in Architecture, ETH Zurich, joined by Supermanoeuvre in Sydney as well as Zwarts & Jansma Architects (ZJA) in Amsterdam.

HiLo introduces several innovations, and this paper relates in particular to the development of a reusable and lightweight cable-net and fabric formwork system to construct the anticlastic, thin shell roof, with no internal falsework. Van Mele and Block [1,2] presented a method for finding the distribution of forces required in such a cable-net or membrane formwork to obtain a particular shape, after it has been loaded with concrete. This control allows a range of pre-defined, non-analytical, anticlastic shapes to be designed and constructed, thus offering room for shape optimization. In 2010, the first author provided consultancy to ZJA for a competition to design an interstate wildlife crossing. In this context, ZJA proposed to use a cable-net supported fabric to push the concept of a flexible formwork to the scale of long-span bridges emphasizing its qualities and constructional advantages [3]. The present paper is a continuation of these earlier ideas.

1.2. Objectives

The objectives of this paper are twofold. First, to establish, as a proof of concept, a complete workflow for the structural design of an anticlastic thin concrete shell taking into account the fabrication constraints of a hybrid cable-net and fabric formwork. Second, to construct prototype shells based on this workflow in order to identify challenges in both computational and constructional aspects. The results of this paper are then used to inform future research and development of the workflow and construction method for full-scale structures in general, and the roof structure of HiLo in particular.

2. Historical overview of related work

The innovations in this and future work are rooted in the longer history of using (prestressed) fabrics as a flexible formwork to construct thin-shell concrete structures. This section serves as a first comprehensive overview of flexible formworks for anticlastic shells. The overview is meant to frame the present research and highlight some of the similarities and differences with our particular approach.

2.1. Fabric-formed shells

The British engineer, James Hardress de Warenne Waller (1884–1968), was the first to apply fabrics to the construction of thin shells. He developed the 'Ctesiphon' system, which started from reusable, lightweight falsework arches, made of steel or timber, catenary in profile, and placed in parallel. A slightly prestressed hessian fabric was tacked to the arches and, under the weight of the applied cement mortar, sagged in between the falsework arches to form corrugations, acting as a lost formwork. The thickness of the first thin coat of cement, the prestress in the fabric and the spacing between the arches would determine the depth of the corrugations, and thus the stiffness of the shell. The system was competitive as it reduced the cost of molds and scaffolding, and required no skilled labor [4].

Waller patented a specific system in 1955 for spans of up to 150 m using prefabricated, external trussed arches from which to suspend the fabric. By the end of the 1970s, the Ctesiphon system had been used around the world for the construction of over 500 shell structures. Two of Waller's last and largest were the Chivas Distillery Warehouses in Paisley, Scotland. The two structures, 100 ft (30.5 m) and 150 ft (45.7 m) long, each featuring three 100 ft (30.5 m) spans, have a thickness of 2.5 in. (6.4 cm), with the fabric spanning 2.54 m between the arches [5] (Fig. 2). The success of the system was partially attributed to the rising demand for unobstructed covered spaces with increased clearances in addition to global shortages at the time of the "modern wonder material, steel", as well as timber [6].

The renowned shell builder Félix Candela Outeriño (1910–1997) used the Ctesiphon system for his first shell, an experimental

Fig. 2. Formwork [5] (top) and current state in 2013 (bottom) of the shell of the Chivas Distillery Warehouse, now Chivas Central Bottling Hall and despatch warehouse, Scotland, ca. 1959, by James Waller et al., with 30.5 m spans and thickness of 6.4 cm. Photo (bottom) courtesy of Chivas Brother Ltd.

vault with a 6m span in San Bartolo, Mexico City and again for a rural school near Victoria, Tamaulipas in 1951 [7].

2.2. Hyperbolic paraboloid shells

After that, Candela moved on to geometries based on the hyperbolic paraboloid (hypar). This is a ruled shape, meaning that although it is doubly curved, it can be described by straight elements. This presented a uniquely efficient way of constructing shuttering made from straight, reusable timber planks (Fig. 3). Although both this and the Ctesiphon system were ingenious construction systems at the time, their disappearance from practice is most likely related to the general decline of shell building. The rising cost of labor and declining price of steel, made shell building less attractive.

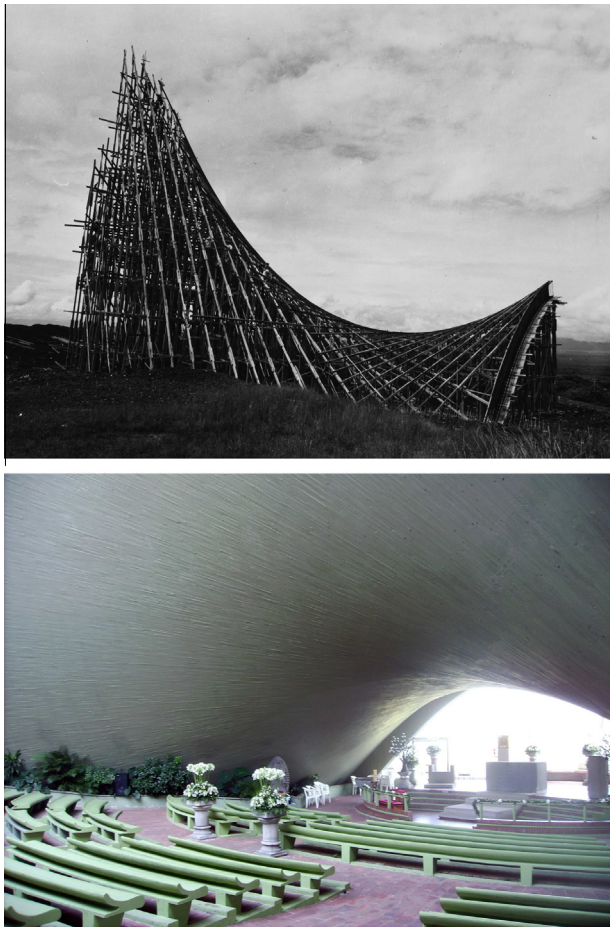

Fig. 3. Falsework (top) and current state in 2008 (bottom) of the shell of the Chapel Lomas de Cuernavaca, Mexico, 1958, by Félix Candela et al. It has a minimum 18 m span and thickness of 4 cm. Photos (top) ©Princeton University Library and (bottom) ©Eduardo Alarcón.

Alternative structural systems to cover large spaces became available through the development of steel and timber gridshells, and more importantly of tensioned membrane structures. In the latter case, the membrane is the structure itself, requiring no formwork and falsework. These systems became possible through the increasing quality, strength and affordability of coated polymer fabrics. At the same time, these fabrics gave rise to new opportunities for fabric-formed concrete [8] and the present method.

2.3. Fabric-formed hypars

An alternative to Candela's system of forming the surface of a hypar is to prestress a fabric, similar to Waller's system. In this way, no heavy timber shuttering and no falsework at all are needed to carry the surface of the shell, as all loads from the fresh concrete are transferred to the boundaries. Such a system was pioneered and patented by Joseph A. Kersavage in the 1970s at the University of Tennessee. Using strips of insect, plastic or metal screen, and later fabric, a hypar surface was formed, which was then bonded by applying a semi-rigid material such as acrylic plastic (Fig. 4a) [9], or by brushing or spraying a mix of latex, cement and sand to a thickness of only 1 cm [10,11]. The formwork system was developed further in collaboration with George Nez and Albert Knott, starting with a 1977 storage building roof consisting of four hypars for the Rocky Mountain Park, and resulting in several other roof structures in the USA. This ultimately led to the successful application of the system in about 20 projects in developed and mostly developing countries, most of which feature arrangements of several hypar shells (Figs. 4b and c). Like Waller's Ctesiphon system, their solution requires low- to unskilled labor with little or no supervision. These roofs have attracted some recent academic interest, investigating the seismic behavior of these structures [12], and the properties of the latex-modified concrete [13].

2.4. Recent fabric-formed anticlastic shells

In 2006, several experiments at Eindhoven University of Technology were intended to demonstrate a proposed construction

(a) Patent by Kersavage [9] (b) First strips applied to frame (c) Hypar hoisted into place

Fig. 4. Latex-modified concrete hypar roofs by TSC Global, Port-au-Prince, Haiti, 2011. Photos (b and c) by Stephen Riley, TSC Global (Creative Commons License CC-BY-NC-SA 2.0).

method using fabric and shotcrete. A 7 m high, 2.5 m wide prototype with a thickness of 7 cm was constructed (Fig. 5a). The project concluded that the construction method would be feasible in a developed country, but that the surface could have deviations as a result of the application of shotcrete, up to several centimeters [14]. A follow-up feasibility report showed an additional experiment replacing the fabric by a stiffer metal mesh to resolve the issue of form control, and mentioned the use of a cable net with rebar for the actual proposed construction method [15].

By 2009, the Centre for Architectural Structures and Technology, or CAST, at the University of Manitoba, Canada, had undertaken several experiments in small- to fullscale fabric formed shell elements; single curved, synclastic and anticlastic shapes, many with local wrinkles corrugating the surface [16].

At the Vrije Universiteit Brussel, a series of ten prototypes were constructed from a prestressed fabric using shotcrete [17,18]. The final shell had a thickness of 5 cm and a 2 m span (Fig. 5b). After applying the shotcrete, the deformed shape was calculated and compared to a numerical model, but for the ten shells, deviations from the expected deflections were measured ranging between 5% and 58%, to more than 100% for non-coated fabrics. These errors were attributed to "slip at the fixation points, and the dynamic effects of the shotcreting".

Yet another independent physical experiment was carried out at the University of Edinburgh, as part of a student project, to investigate constructional aspects of the fabric forming of a hypar shell [19]. The work is unpublished at present, but briefly shown by Brennan et al. [20] (Fig. 5c).

2.5. Discrete flexible formworks

An alternative tensile formwork system is to replace the fabric by discrete elements, such as the system briefly shown by De Bolster et al. [21] in the context of hypar shells. This reusable and reconfigurable 'cable net' was proposed by Mollaert and Hebbelinck [22] and was in fact constructed as a network of edge chains and adjustable belts. The network was covered with EPS tiles before applying a fiber-reinforced mineral polymer on either side (unpublished work by Sven Hebbelinck).

A similar, older system is the "offset wire method" (OWM), developed by Waling and Greszczuk [23] at Purdue University, Indiana, USA. The method used two layers of wires to sandwich a layer of EPS tiles on top of which concrete could be cast. This generated a hypar shell, whilst avoiding the need for "a forest of falsework".

After building a 37 7/8 in. (1 m) square small-scale model, they proceeded with a large-scale 20 ft (6.1 m) square laboratory model with a rise of 7 ft (2.1 m). The shell had 3 in. (7.6 cm) thick EPS designed for a 2 in. (5.1 cm) thick concrete cover, deviating by 2.7 in. (69 mm) from a true hypar at its center. A coating of mortar reduced deflections to 0.43 in. (11 mm), but showed cracking above 80% of the applied load. The wires, spaced 12 in. (30.5 cm), and prestressed up to 600 lb (2.7 kN) using "standard prestressing equipment" [23].

As a result of these experiments, two 64 ft (19.5 m) square buildings were soon successfully completed; the Bay Refining Gas Station and Carwash in Midland, Michigan [24], and the clubhouse at the Purdue Golf Course in West Lafayette, Indiana [25] (demolished in the mid-1990s), both an assembly of four hypars (Fig. 6). The Purdue shell had two layers of 0.135 in. (3.4 mm) wires, 6 ft (1.8 m) offset from the straight line generators. The bottom wires were spaced 12 in. (30 cm) apart, the top layer 24 in. (60 cm) apart. The shell used 3 in. thick EPS foam, a 0.5 in. stiffening mortar, a 3 in. concrete cover and traditional rebar, 16.5 cm in total.

3. Methodology

To fully realize the structural efficiency of a flexibly formed shell, it is crucial to both design an optimal shell within the project's constraints and to control the cable forces such that its form, despite the formwork's flexibility and the weight of the wet concrete, is in the end exactly as required. A computational approach to realize this goal was developed and is explained in this section in more detail. The procedure is shown in Fig. 7, and consists of eight steps:

1. establishing the boundary conditions (Section 3.1) and target shape of the shell (Section 3.2);
2. generating a cable-net topology and mapping it onto the surface (Section 3.3);
3. patterning of the surface for the fabric (Section 3.4);
4. computing the nodal target loads based on the target shape and thickness (Section 3.5);
5. best-fit optimization of the cable forces under load in the final state (Section 3.6);
6. materialization of the cables (Section 3.7);
7. determination of the cable forces prior to casting through static analysis of the unloaded cable net (Section 3.8); and
8. design of the external frame that ensures the chosen boundary conditions (Section 4.1).

Calculations for loading cases other than the design loading (self-weight of the formwork and concrete) need to be carried out afterwards to further check the design, although they could potentially be integrated in step 1 for the shell and step 7 for the cable net.

3.1. Boundary conditions and initial shape

As a starting point, the boundary conditions and initial shape of our shell are based on a 'simple' hyperbolic paraboloid (hypar)

(a) Eindhoven, 2006. Photo by Arno Pronk

(b) Brussels, 2009. Courtesy of N. Cauberg (WTCB), D. Janssen (Centexbel), M. Mollaert (VUB)

(c) Edinburgh, 2012. Courtesy of Barnaby Ghaui and Meagan Graham, ESALA.

Fig. 5. Recent hypar shells using flexible formwork.

Fig. 6. Laboratory model, formwork and completed state of the Purdue Golf Clubhouse, Indiana, USA, ca. 1962, by J.L. Waling et al., has a minimum 13.8 m span and 8.9 cm (structural) thickness. Reprinted with permission from [25] by the National Academy of Sciences. Courtesy of National Academies Press, Washington, D.C.

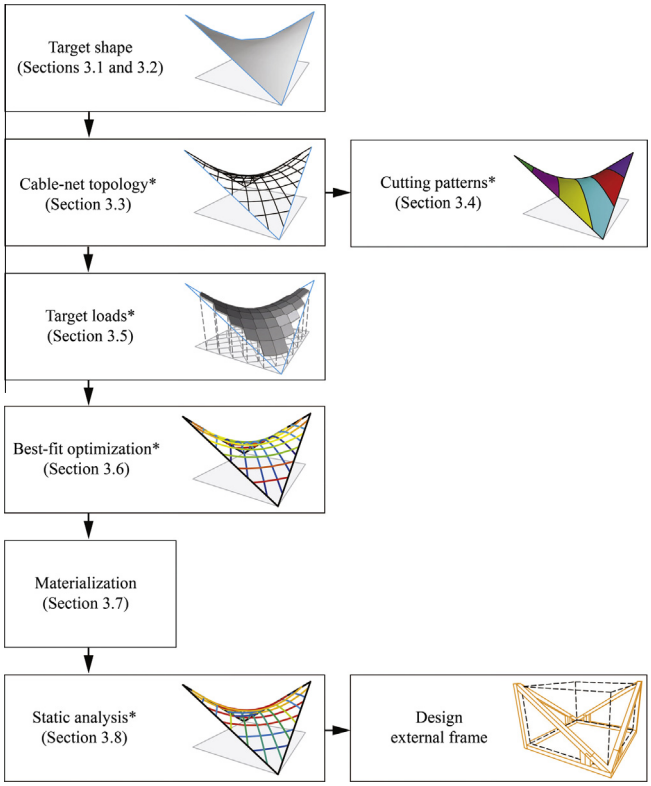

Fig. 7. Outline of the computational procedure (*indicates iterative procedure; the target shape can be iteratively determined or given by the designer).

with a square plan, with the bounding box measuring $w \times b \times h = 1.8\,\text{m} \times 1.8\,\text{m} \times 1.2\,\text{m}$ (Fig. 8) and a thickness of between 1.5 and 2.5 cm (to be determined). For a set of given x- and y-coordinates, the heightfield of the hypar is described by

$$z = c\left(\frac{y^2}{b^2} - \frac{x^2}{a^2}\right)$$

where a, b, and c are parameters determining the shape. For a symmetric hypar with straight edges within our bounding box, $a = b = 1$ and $c = h/w^2 = 1.2/1.8^2 = 10/27$. In the rest of our design process, these straight boundaries are kept fixed, for simplicity of our initial prototypes.

Eventually, when the shell has cured and the formwork is removed, the lower supports each have four constraints; three translations and one rotation (Fig. 9). The shell has no edge beams and (approximately) uniform thickness. For single or arrangements of four hypars, reducing or entirely removing any edge beam (possibly thickening the shell at the supports) decreases overall shell bending [26,27]. Although maximum displacements may increase, they are not significant compared to serviceability limits.

3.2. Target shape

Although some of the thinnest known shell structures are hypars, very slight improvements to their geometry can drastically improve their structural behavior [28]. However, their formwork can then no longer be described by straight elements, whereas a flexible formwork can accommodate these changes as long as the shape remains anticlastic. Subject to this condition, the target shape for the cable net can be any given shape. In this case, as part of our conceptual design process, structural shape optimization is applied. Our objective is to minimize the maximum deflection and thus optimize the stiffness.

Research at the Vrije Universiteit Brussel, subsequent to that of Cauberg et al. [17], described the form finding of such flexibly formed, anticlastic shells using FDM [29] and DR [30], both

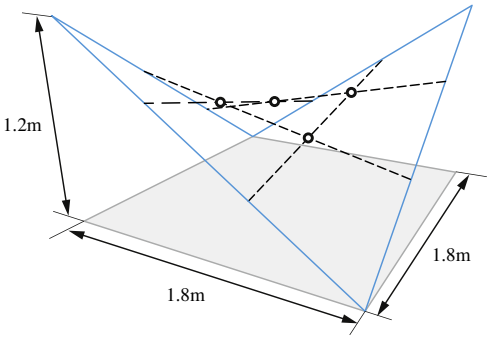

Fig. 8. Boundary conditions and NURBS control points, allowed to move vertically within the bounding box while maintaining anticlasticity.

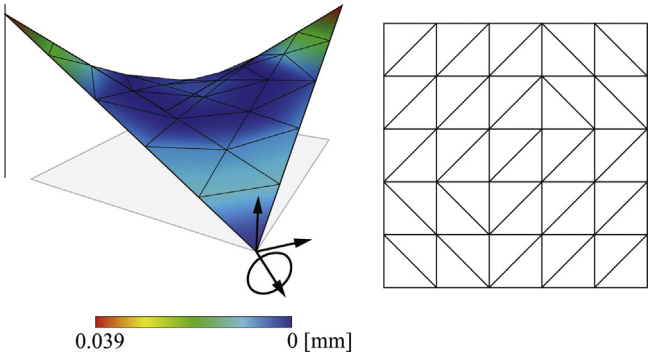

Fig. 9. FE mesh with TRIC-elements and support restraints.

modelling them as discrete networks under a given selfweight of the concrete. A set of two force densities (corresponding to the two orthogonal directions) or a (fictitious) elastic stiffness (identical for all links) were varied to obtain a shape that fitted some spatial requirements of the designer. Guldentops et al. [29] also compared such a form to that of a hypar of similar (but not identical) size and boundary conditions, showing deflections to be lower. However, to reduce deflections even more, we apply shape optimization instead of form finding.

Bletzinger et al. [31] suggested to use a form-finding method as a shape generator for structural optimization by varying the loads (distribution of selfweight). However, compared to varying geometric parameters (e.g. control points of the surface), they demonstrate that results are less optimal (for uniform thickness), since the degrees of freedom are reduced. This leads us to choose a geometric parameterization, using a NURBS surface, for the time being (Fig. 8). The control points of the NURBS surface are allowed to move vertically within the bounding box of our boundary conditions, such that the resulting geometry never becomes synclastic. The shape is optimized using a genetic algorithm by varying the control points [32].

When optimizing a shape to achieve the lowest maximum deflection (serviceability limit state), with self-weight as design loading, we expect the material to stay within its elastic range. Therefore, as long as no stress limits are exceeded, we can apply a linear elastic model. Since the present project uses a custom concrete mix design, and does not include material testing, optimization is carried out for the probable limits of linear elastic stiffness. Based on Eurocode strength classes, from regular C25/30 to high-strength C90/105, the linear elastic stiffness E of the concrete might vary between 31 GPa and 44 GPa. The results show that the stiffness, within this range, does not significantly influence the shape. The model's thickness is designed to be in the range of 1.5–2.5 cm, so we optimize for both of these limits as well (Table 1).

In summary, we minimize the maximum deflection by varying the vertical position of the four control points within the bounding box of the boundary conditions. The problem is not subject to any other constraints, since displacements are very low and additional load cases are not considered at this stage.

The FE software used (see Section 3.9) provides one type of shell element, that is described as being similar to the TRIC-element [33], which already produces accurate results for doubly curved geometries at coarse meshes, avoids any shear locking [34] and neglects transverse shear deformation [35] meaning that it applies to thin shells.

Table 1 shows the results from optimization compared to the initial hypar. We observe that the relative reduction in deflections increases with shell thickness, and thus the influence of flexural behavior. The shape for the lower bound uniform thickness of 1.5cm is chosen for further development (Fig. 9).

3.3. Cable-net topology design

The next step, having settled on the required shape of the shell, is to map a cable net onto the surface that serves as the main load-bearing and shape-defining part of our flexible formwork system. Several criteria govern the design of the cable-net topology:

- The valency of the cable net should generally be even to allow, for practical reasons, continuous cables up to the boundaries.
- Continuous cables should terminate at the boundaries to allow for more convenient prestressing (and thus control) throughout, rather than loop within the mesh.
- Continuous cables should follow principal curvatures of the surface to reduce the amount of prestressing required, as the cables' load capacity is proportional to prestress and curvature.
- Continuous cables should have as low geodesic curvature as possible, if they are to serve as guides or seam lines for secondary fabric strips or cutting patterns (thus reducing material waste).
- The density of the mesh should be fine enough such that the demands on the secondary fabric are low (in terms of strength, prestressing and patterning requirements).
- The density of the mesh should be coarse enough, such that the total length of cable, the number of intersections and the amount of prestressing work (thus material and labor cost) are reduced.

Given these considerations, we start by roughly orienting a quad mesh along the lines of principal curvature (Fig. 10a). The end points are used to plot geodesics along the surface of the shell, corresponding well with principal curvature (Fig. 10b). Then, the end points are moved to optimize the mesh width (Fig. 10c). The objective is to reduce the standard deviation of the mesh width. By moving the end points, the total number of nodes along the boundary increases, but in terms of construction, this simplifies matters, since at each point, only one cable now terminates. We set our mesh width at approximately 20 cm with a 30 cm upper limit. Table 2 shows the result of the manual optimization.

3.4. Cutting patterns

As discussed, aligning the seam lines of cutting patterns along geodesics minimizes waste. The cables, already geodesic, are chosen as seam lines, and the surface in between is unrolled using an area-preserving approach. The surface is subdivided, triangulated and flattened. The degree of subdivision is increased until the difference between surface areas of the flattened pattern and the original doubly curved surface are within a certain tolerance, in our case 0.01 m^2 (Fig. 11).

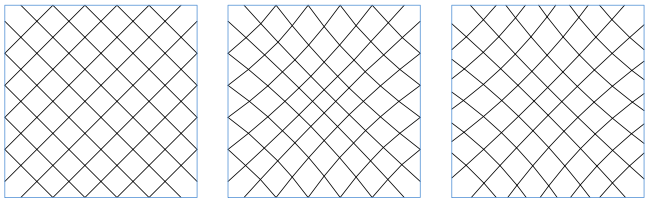

(a) Quad mesh (b) Initial geodesics (c) More uniform mesh

Fig. 10. Optimization of the cable-net geometry.

Table 1
Results (height at midspan) and fitness (max. deflection at the tips) of shape optimization, identical for C25/30 and C90/105.

	Thickness (cm)	Height at midspan (cm)	Deflection at tips (mm)
Hypar	1.5	60	0.079
Optimized	1.5	62	0.078
Hypar	2.5	60	0.040
Optimized	2.5	78	0.037

Table 2
Mean, minimum and maximum mesh width, and standard deviation, in (cm).

	Mean	Min.	Max.	St. dev.
Initial	21	15	28	4
Optimized	23	18	26	2

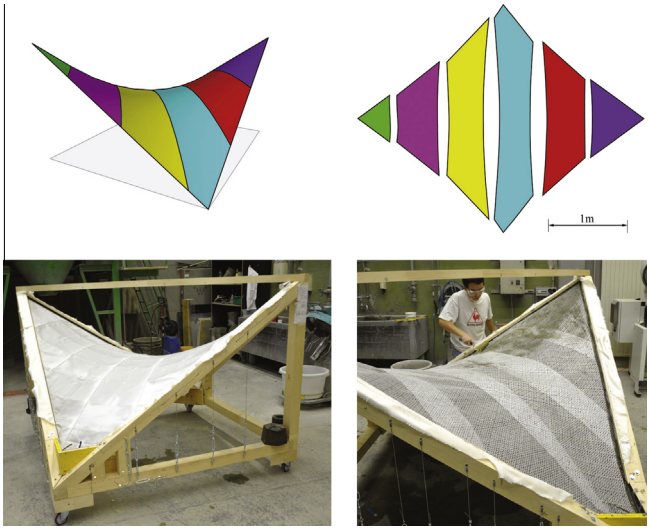

Fig. 11. Cutting patterns, cut along cable lines, used for the fabric shuttering and the textile reinforcement of the second prototype.

Of the two directions in the net, the standing cables are chosen for the seams, such that the fabric strips can simply be placed over the cable net without the possibility of sliding down. The patterns are designed to skip every other cable, to compare the effect on the concrete imprint. For engineered membrane structures, the cutting patterns are shrunk to compensate for the prestress, such that the resulting surface is properly tensioned and smooth. In our case, for simplicity of construction and aesthetic reasons, the patterns are not compensated, such that the unstrained fabric sags between the cables once the concrete is applied.

3.5. Target loads

To determine the forces in the cable net, we first calculate the target loads on the nodes of the net as an approximation of our target shape. Each load is assumed to be the tributary area of a corresponding node in the net, extruded by the average thickness of the shell. Although the shape is optimized for 1.5 cm, the thickness for the load calculation is changed to 2.5 cm to accommodate the expected sag of the fabric. This means the additional thickness is assumed to act as dead load, but not contribute structurally to the shell. First, the Voronoi diagram of the projected cable-net nodes is determined. The cells are projected onto the target surface, planarized and then extruded normal to the surface by the assumed thickness. The density is set to 24 kN/m^2.

3.6. Best-fit optimization

We wish to find the required cable-net forces such that, under given loads of the wet concrete, the resulting concrete shell takes the form of the target shape. As mentioned, this problem has already been addressed and solved by the second author through a non-linear extension of thrust network analysis (TNA) [2]. This approach used the Levenberg–Marquardt algorithm (LMA) as a least-squares solver, which interpolates between the Gauss–Newton algorithm (GNA) and the method of gradient descent. For the sake of comparison (see Section 5), non-linear extension of the force density method (FDM) [36,37] is implemented and adapted to our problem. The approach uses GNA as a least-squares solver.

The goal is to minimize changes in coordinates $\Delta\mathbf{x}_N$, $\Delta\mathbf{y}_N$, $\Delta\mathbf{z}_N$ and force densities $\Delta\mathbf{q}$, such that the coordinates $\mathbf{x}$, $\mathbf{y}$, $\mathbf{z}$ approach the target shape, while satisfying static equilibrium. The results are the force densities $\mathbf{q}$ or forces $\mathbf{f}$ required after casting of the concrete.

Using a branch-node matrix $\mathbf{C}$ to describe the topology of the cable-net of m cable segments and n nodes, the coordinate differences for all m cable links are $\mathbf{u} = \mathbf{C}\mathbf{x}$, $\mathbf{v} = \mathbf{C}\mathbf{y}$, and $\mathbf{w} = \mathbf{C}\mathbf{z}$ [38]. The branch-node matrix and the coordinate vectors are split in two based on the $n = n_N + n_F$ free and fixed nodes: $\mathbf{C} = [\mathbf{C}_N \quad \mathbf{C}_F]$, $\mathbf{x} = [\mathbf{x}_N \quad \mathbf{x}_F]$, $\mathbf{y} = [\mathbf{y}_N \quad \mathbf{y}_F]$ and $\mathbf{z} = [\mathbf{z}_N \quad \mathbf{z}_F]$. We can define static equilibrium in each direction as

$$\mathbf{C}_N^T\mathbf{U}\mathbf{q} = \mathbf{D}_N\mathbf{x}_N + \mathbf{D}_F\mathbf{x}_F = \mathbf{0} \tag{1}$$

$$\mathbf{C}_N^T\mathbf{V}\mathbf{q} = \mathbf{D}_N\mathbf{y}_N + \mathbf{D}_F\mathbf{y}_F = \mathbf{0} \tag{2}$$

$$\mathbf{C}_N^T\mathbf{W}\mathbf{q} - \mathbf{p} = \mathbf{D}_N\mathbf{z}_N + \mathbf{D}_F\mathbf{z}_F - \mathbf{p} = \mathbf{0} \tag{3}$$

where, to simplify notation, $\mathbf{D}_N = \mathbf{C}_N^T\mathbf{Q}\mathbf{C}_N$ and $\mathbf{D}_F = \mathbf{C}_N^T\mathbf{Q}\mathbf{C}_F$. The matrices $\mathbf{U}$, $\mathbf{V}$, $\mathbf{W}$ and $\mathbf{Q}$ are the diagonal matrices of vectors $\mathbf{u}$, $\mathbf{v}$, $\mathbf{w}$ and $\mathbf{q}$.

This is rewritten as a single system

$$\mathbf{A}\mathbf{q} - \bar{\mathbf{p}} = \overline{\mathbf{D}}_N\bar{\mathbf{x}}_N + \overline{\mathbf{D}}_F\bar{\mathbf{x}}_F - \bar{\mathbf{p}} = \mathbf{0} \tag{4}$$

where $\overline{\mathbf{D}}_N$ and $\overline{\mathbf{D}}_F$ are block diagonal matrices, and remaining vectors and matrices are vertically stacked.

We linearize Eq. (4) with respect to the unknowns $\mathbf{q}$ and $\bar{\mathbf{x}}_N$ and obtain [39]:

$$\begin{bmatrix}\overline{\mathbf{D}}_N & k\mathbf{A}\end{bmatrix}\begin{bmatrix}\Delta\bar{\mathbf{x}}_N \\ \Delta\mathbf{q}\end{bmatrix} = \bar{\mathbf{p}} - \mathbf{A}_0\mathbf{q}_0 \tag{5}$$

where weighting factor k was set to 10 in our case. This is an underdetermined system of equations, since the left-hand side matrix is $3n_N \times (3n_N + m)$. Such a system can be solved with a least-squares solver such as GNA. In each iteration i, one sets $\mathbf{q}_{i+1} = \mathbf{q}_i + \Delta\mathbf{q}$, then updates $\mathbf{D}_N$ as well as the residuals, and repeats the iteration until convergence is reached, in our case if $\|\Delta\bar{\mathbf{x}}_N\| < \epsilon = 0.001$, occurring after 707 iterations (22 s). Upon convergence, the required prestresses under the load of the fresh concrete can be calculated by simply multiplying the force densities with the lengths of the cable links.

Fig. 12 shows the results for an orthogonal net, one based on OWM (see Section 2.5) and one aligning with principal curvatures, each mapped onto our target surface. Note that the first cable net would have infinite forces on a hypar, but for the optimized shape has a slight curvature, allowing us to find a solution.

3.7. Materialization

Having determined the forces after casting in Section 3.6, we wish to know the forces prior to casting in order to construct and prestress our formwork. To do so, we materialize and dimension the cable net. The smallest steel cable available to us is 2 mm INOX with a tensile strength of 3.7 kN. This is well above the maximum tensile stress after casting (factor of 13.5). The stiffness of our cable

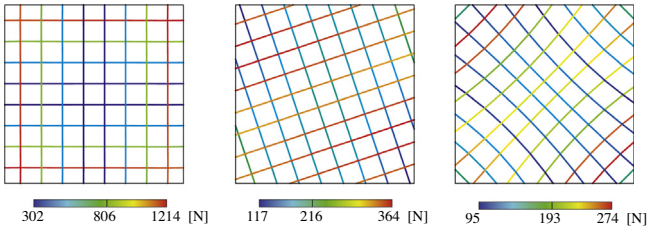

Fig. 12. Cable forces after casting from best-fit optimization, where aligning with principal curvatures reduces the required prestress.

is not specified by the manufacturer, but presumably it is $E = 195\ \mathrm{N/mm^2}$ based on the relevant German DIN-norm.

So, having chosen a material and cross-section, with an axial stiffness $EA = 195\pi$, the initial lengths $\mathbf{l}_0$ can directly be computed from the forces $\mathbf{f}$ and lengths $\mathbf{l}$ in the final state [40]:

$$\mathbf{l}_0 = \left(\mathbf{I} + (\mathbf{EA})^{-1}\mathbf{F}\right)^{-1}\mathbf{l} \tag{6}$$

where $\mathbf{I}$ is an identity matrix of size m, and $\mathbf{EA}$ and $\mathbf{F}$ are diagonal matrices of all stiffnesses EA and the forces $\mathbf{f}$ respectively.

3.8. Static analysis

From the final state geometry, and the newly given stiffnesses and resulting initial lengths, it is now possible to compute the intermediate geometry and forces prior to casting. In that situation, the fresh concrete has not been applied yet, so assuming the selfweight of the formwork to be negligible compared to the prestresses, we simply remove the loads when computing the residual forces and attempt to find a new equilibrium shape. This FE analysis is performed using dynamic relaxation [41] (this method is well-known as a form-finding method, but here we used real material values, making it equivalent to FE analysis with a particular type of element and solver).

After dynamic relaxation, we obtain new lengths and recompute the forces. The cables were dimensioned for the forces after casting and Fig. 13 shows that, as expected, the range of forces has decreased for the unloaded state.

3.9. Implementation

The procedure, outlined in Fig. 7, was implemented in Grasshopper for Rhinoceros, using its built-in Galapagos components for the genetic algorithm, plug-ins Karamba to evaluate deflections, and Kangaroo for the dynamic relaxation. In addition, custom Python components were written in IronPython, using the NumPy library. NumPy functions used were `numpy.linalg.inv` (which uses Lapack's subroutine `DGESV`, based on LU factorization), to solve linear systems such as in Eq. (6), and `numpy.linalg.lstsq` (which uses Lapack's subroutine `DGELSD`) to solve the least squares problem in Eq. (5) using singular value decomposition (SVD). Because NumPy algorithms for sparse matrices are not implemented in IronPython, the ALGLIB library for IronPython was later used to solve sparse least squares problems with `xalglib.linlsqrsolvesparse`, based on the LSQR algorithm. Unrolling of the surface to create cutting patterns was achieved by adapting a Grasshopper definition by Andrew Heumann.

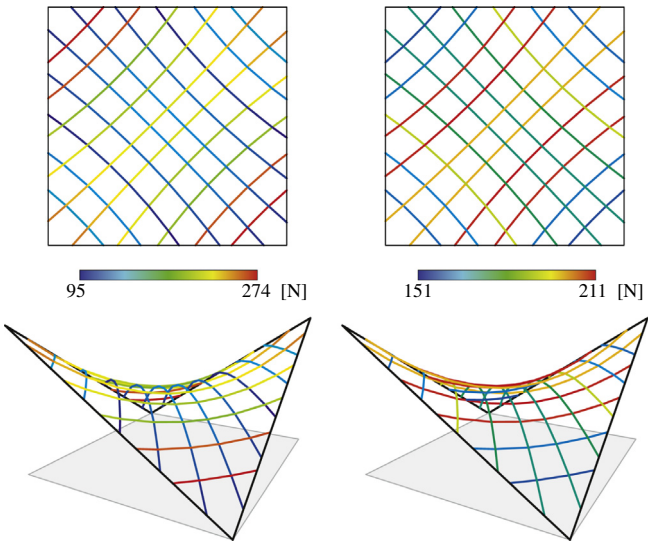

Fig. 13. Cable forces after and before casting. The range of prestress is smaller in the latter state.

4. Results

Based on the computational approach presented in the previous section, two prototype shells were built as a proof-of-concept.

4.1. External frame

A timber frame was built to follow the boundaries of the shell and resist the applied prestresses, using 9 cm square fir elements (Fig. 14). The frame was designed such that the upper part would be removable for demolding, whilst the lower part would support the two bottom corners of the hypar. A tension tie connected the two bottom corners to resist the horizontal thrust from the shell. Because the frame edges might deflect due to bending in the order of 1 mm (based on calculations), it was decided during construction to add an additional timber cross, connecting the midpoints of the frame edges (see Fig. 14, right) and a top member for the second prototype (to allow access for measurements).

4.2. Cable net and prestress

The cable net was made from 2 mm stainless steel cable. Cables were guided through the timber frame along cringles, terminating at eyebolts using crimp sleeves. For the first prototype, nodes were fixed by winding a piece of wire around the intersecting cables. For the second, cross clamps were used instead (Fig. 15), which also served as measuring points for photogrammetry.

At one end of each of the twenty cables, a turnbuckle was used to introduce prestress. The prestressing was controlled by measuring the lengths of the cable segments during prestressing, attempting to approach the digital model as closely as possible. Prestressing was then further refined by measuring and checking the forces in several cable segments. In the first prototype, this was done by measuring the elongation of springs at twenty locations inside the net. For the second prototype, a portable cable tension meter was used instead, allowing more measurements of higher accuracy.

4.3. Fabric

The first fabric was a PP geotextile, Propex 60-7041, with a tensile strength of 42 kN/m, and a 5.2 m roll width. The geotextile was chosen purely for its similarity to the North American Propex 315ST, used by Prof. Mark West in many of his experiments at C.A.S.T. It is very similar in weight, strength and hydraulic properties.

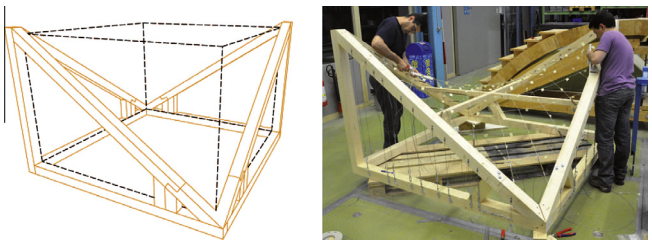

Fig. 14. Design and photo of the first prototype, with a cross added in the as-built frame.

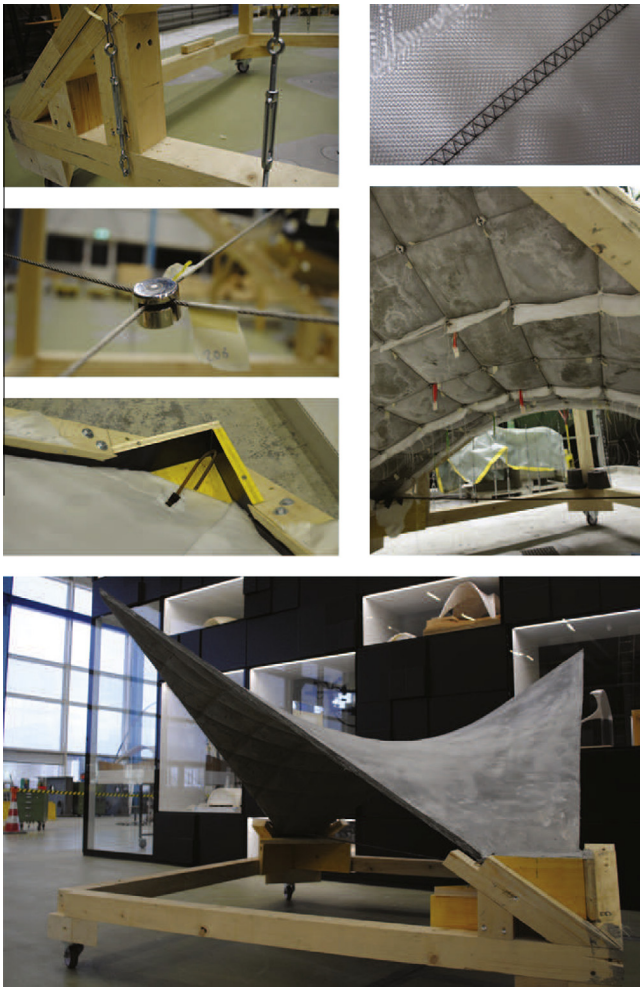

Fig. 15. Construction of the second prototype (clockwise from top left): turnbuckles, stitched seam, surface after casting, final result, corner support detail, and node with cross clamp.

The second fabric was a PP Proserve F0899 with a tensile strength of 54–60 kN/m, and 3.6 m roll width, used for underwater fabric formworks. The fabrics were tacked onto the timber frame. The second fabric was also clamped to the frame with an additional timber profile to control the edge geometry.

4.4. Concrete

After prestressing the net, the fabric was applied and a 0.9–2.9 cm (average ca. 2.4 cm, see Fig. 16) thick layer PVA fiber reinforced cement mortar was hand-rendered on top. The second shell was cast while continuously measuring the thickness for better control, by distributing the concrete accordingly. It was also fitted with an additional layer of AR-glass textile reinforcement. The mix design and choice of fiber reinforcement was adapted from Máca et al. [42] based on further discussion and availability of materials

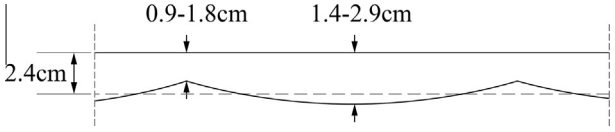

Fig. 16. Diagram of varying shell thickness for the first prototype due to undulations between cables (not to scale).

at our concrete lab. The mix design was not the focus of our present research, so the only criteria were to obtain a mixture with high slump, resistance to shrinkage cracking and tensile capacity. The proportions by weight were:

- 1 kg cement (Holcim Normo 5R, CEM I 52.5).
- 0.1 kg microsilica (Elkem Grade 971-U).
- 0.7 kg fine sand/aggregate (0/4 mm).
- 0.015 kg PVA fibers (Kuralon K-II 6/12 mm).
- 0.24 l water.
- 0.010–0.015 l plasticizer (BASF Glenium ACE 30).
- 0.015 kg stabilizer (Sika 4R).

4.5. Construction

Construction of the first prototype took place in April, 2013 (Fig. 17). The second prototype was cast in February, 2014. Apart from the initial woodwork, it involved only unskilled labor. The various activities are summarized in Table 3.

4.6. Cost estimation

Table 4 shows the materials and their costs for the first prototype formwork. The cost of the formwork is CHF 527.79, or CHF 162.90 per plan square meter with nearly 60% due to the timber frame. We expect that the relative cost will go down at larger

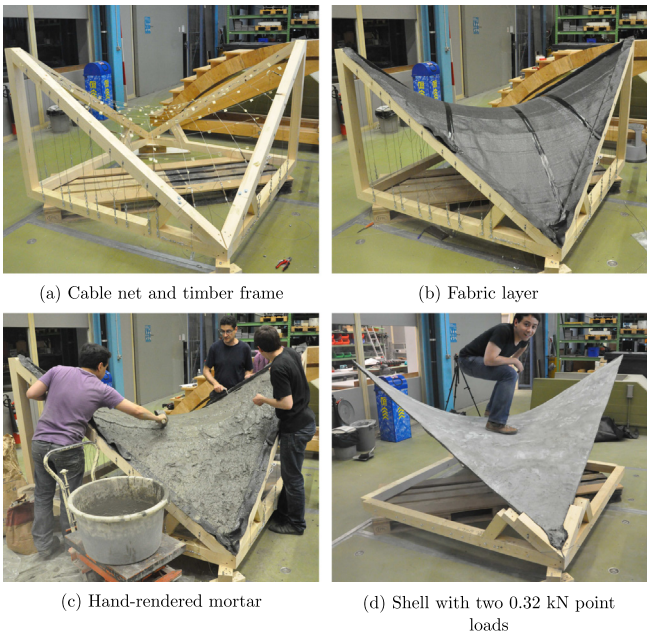

(a) Cable net and timber frame (b) Fabric layer

(c) Hand-rendered mortar (d) Shell with two 0.32 kN point loads

Fig. 17. Construction of the first formwork and shell.

Table 3
Labor involved in constructing , and adapting and reconstructing the formwork.

Activity	Prototype 1 (hours)	Prototype 2 (hours)
Woodwork	8	1
Carpentry	39	15
Installation	34	32
Prestressing	12	14
Patterning	8	5
Concreting	22	14
Total	123	81

Table 4
List of materials, quantities and cost in CHF for the first formwork.

Component	Type	Qty.	Cost per unit	Total excl.	Total cost
Timber	100 × 100 fir	25 m	11.50	287.50	310.50
Fabric	Propex 60-7041	9 m^2	0.71	6.39	7.60
Tacks	1.8 × 20 mm	0.5 kg	26.10		13.05
Cable	INOX V4a 2.0 mm	100 m	0.52	52.29	58.10
Wire	Steel wire 1 mm			12.00	12.96
Cringle	6 mm	60	0.62	37.26	40.24
Turnbuckle	M5	20	2.00	40.00	43.20
Crimp sleeve	2 mm	60	0.09	5.49	5.93
Quick link	4 mm	40	0.56	22.32	24.11
Eye screw	M6 × 40	20	0.56	11.20	12.10
Total					527.79

spans, where the ratio of surface to edge is higher, and for multiple use, since much of the first prototype was reused for the second.

4.7. Measurements and accuracy

After the first shell had hardened, thirteen measurements were taken at nodes of the cable net to see how much the actual prototype deviated from the computer model. Measurements using ruler and laser level revealed an average deviation $\mu = 22$ mm with a standard deviation of $\sigma = 1$ mm. The second shell was made to improve the method of measuring forces and geometry as the main source of error. Forces were measured using a Tensitron ACX-250-M portable cable tension meter, while photogrammetry was used to register nodal positions. The cable net was loaded using weights of sand equivalent to the nodal loads in the computer model. This also meant that the cables remained accessible in the loaded state, allowing measurements of forces. The resulting average deviation from the target surface $\mu = 2.0$ mm with a standard deviation of $\sigma = 1.5$ mm.

Table 5 and Fig. 18 show an overview of our two as well as precedent prototypes for which data was published. Here the total difference between design model and final loaded state are compared, where the difference is the sum of deformations due to loading and deviations between theoretical and physical model. The proposed design procedure accounts for the final loaded state of the formwork, so the second prototype is particularly accurate by comparison. In general, good results were obtained in each study, considering the inherent flexibility of these formworks.

5. Discussion

A historical investigation yielded a large number of precedents of flexibly formed, anticlastic shell structures. A recurring topic among these works is the lack of control of deviations. Based on

Table 5
Comparison of deformations and deviations, relative to the span, in flexible formworks.

Ref.	Surface	Eq. thickness in concrete (cm)	Span s (m)	Plan (m)	Deformation δ due to loading (mm)	Deviation Δ from theoretical (mm)	Rel. difference $\frac{\delta+\Delta}{s}$ (‰)
[23]	Cable + EPS-foam	3.5	1.4	1 × 1	18	5	16
	Cable + EPS-foam + mortar	4.0	8.6	6.1 × 6.1	69	13	8.0
		4.6	8.6	6.1 × 6.1	11	13	2.8
[17]	Coated PP, PE, PVC	3.6–5.0	2	2 × 2	15	0.75–8.7 (5–58%)	7.9–11.9
	Uncoated PP, PE, PVC					⩾15 (⩾100%)	⩾15
[Present paper]	Cable + uncoated PP	2.4	2.55	1.8 × 1.8	N/A	22	8.7
	Cable + uncoated PP	1.5				2	0.8

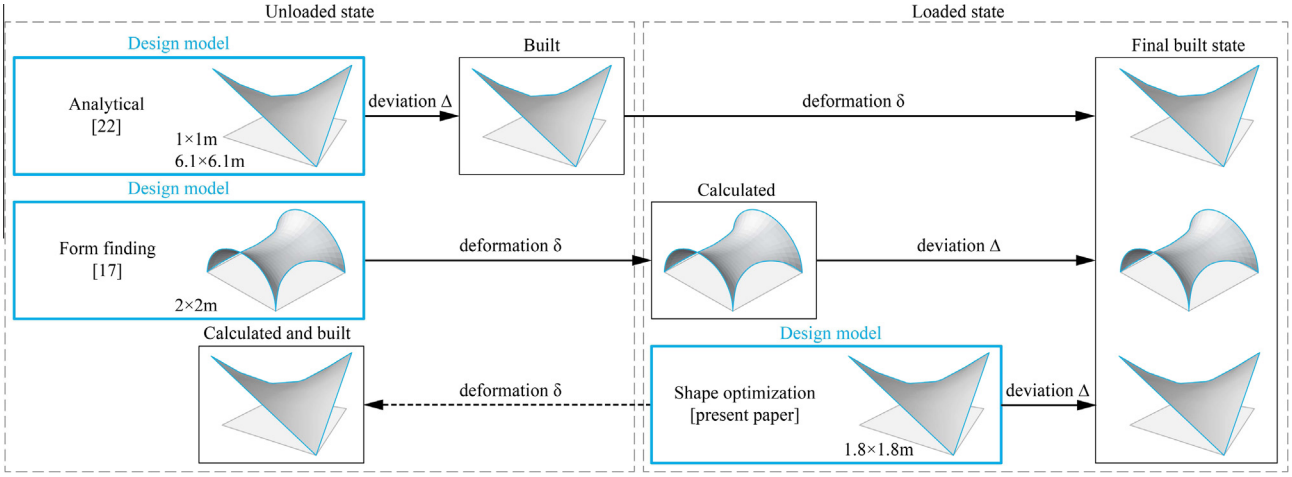

Fig. 18. Sequence of differences from design model to final built state for Table 5.

this historical overview and our own study, possible strategies to improve accuracy are:

- to reduce the applied loading by layering and curing the shell in stages, thereby creating a partially or entirely self-supporting structure as soon as possible;
- to increase the stiffness of the material (e.g. coated instead of uncoated fabrics, cable nets) and/or the prestress such that the formwork is less sensitive to inaccuracies of the applied load;
- to design for the loaded state to exclude deformations from the final comparison; and
- to accurately measure and correct the required prestresses.

Our approach is based on the latter three: a cable net for which we calculate the prestresses required in the final state, then measure and control the prestresses required in the initial state. In this paper, we adapted a non-linear FDM for the calculation of the final state. Its convergence was slow, but satisfactory for the present model. However, some preliminary numerical experiments with more complicated shapes have shown that non-linear FDM tends to diverge, making it unsuitable for future work in its current form. In the method by Van Mele and Block [2] convergence is vastly improved by reducing and controlling the amount of unknowns: first by solving vertical equilibrium separately, and second by identifying m_i independent sets of the m unknown force densities. In other words, the amount of unknowns decreases from $3n+m$ to $n+m_i$, where $m_i \leqslant m$, and n are the number of free nodes.

In further work, the objective will be to scale up the construction method.

In terms of computation, thickness in addition to shape optimization will be included as well as stress constraints when checking for multiple load cases based on Swiss building code and wind modelling. The material model will be updated based on results from material testing of the textile and fiber reinforced concrete.

In terms of construction, the timber frame and turnbuckles will be replaced by steel and jacks. Development of the steel details and prestressing strategy will be an important focus. Partially leaving the frame as a permanent edge beam will be evaluated, depending on results from shape and thickness optimization, as well as based on non-structural considerations.

Finally, the full-scale project will serve as an enclosure, and therefore integrating the structural shell with building systems and insulation while retaining its thinness is another important aspect of the overall design.

6. Conclusions

The field of fabric formwork represents over a century of exciting inventions and discoveries, yet provides many opportunities still. A historical overview of flexibly formed shell structures and prototypes, often hypars, has been presented, many of which were constructed with comparable goals to the present work. Our proposed solution has been developed to allow large-span formworks with little or no falsework and enable a wider range of anticlastic shapes than those possible through traditional means.

The first prototype presented here is the first cable-net and fabric formwork, and an important step towards a new cable-net and fabric formed roof to be built in Switzerland. Our main contribution is a complete computational design workflow for the prototype shell and its required formwork.

This includes

- the formulation of design criteria for the cable net and its topology;
- the concept of calculating prestresses in the final state, and materializing before finally calculating prestresses prior to casting;
- the design and construction of two prototypes with a discussion on their accuracy.

It is clear that much work needs to be done for the further development of this construction method. However, the present research has enabled us to identify which particular aspects warrant our immediate attention. Future work will focus on improving the optimization procedure and tackling the challenges associated with scaling up the construction method.

Acknowledgements

The authors would like to thank Regine van Limmeren, Masoud Akbarzadeh and Ramon Weber as well as Mile Bezbradica, Jonas Sundberg and David López López for the construction of the two prototypes respectively. David Novák and Prof. Konrad Schindler assisted with the photogrammetry. Further support at ETH Zurich was provided by Oliver Zgraggen, Paul Fischlin, Heinz Richner and Thomas Jaggi. We acknowledge our former students Paul Mayencourt and Matthias Amstad, who worked on a previous formwork.

We especially thank Manuela Tan, and Noah Nichols from Propex as well as Kaloyana Kostova and John Orr from the University of Bath for sponsoring the two fabrics; Jennifer Stevenson, Chivas Brothers Ltd., for providing current photos of the Paisley warehouses; Charlotte Erdmann, Engineering Library of Purdue University, for identifying the Bay Service Station and securing additional copyright permissions; and George Nez and Brad Wells, TSC Global, for information regarding their hypar shell roofs.

References

[1] Van Mele T, Block P. A novel form finding method for fabric formwork for concrete shells. In: Proceedings of the international association for shell and spatial structures symposium 2010. Shanghai, China; 2010.
[2] Van Mele T, Block P. Novel form finding method for fabric formwork for concrete shells. J Int Assoc Shell Spatial Struct 2011;52(4):217–24.
[3] Torsing R, Bakker J, Jansma R, Veenendaal D. Large-scale designs for mixed fabric and cable-net formed structures. In: Orr J, editor. Proceedings of the 2nd international conference on flexible formwork. Bath, UK; 2012. p. 346–55.
[4] Billig K. Concrete shell roofs with flexible moulds. J ICE 1946;25(3):228–31.
[5] Anon. Curved roofs of large span. Concr Constr Eng 1959;54(5):171–4.
[6] Waller JdW, Aston A. Corrugated shell roofs. ICE Proc – Eng Div 1953;2(4):153–82.
[7] Faber C. Candela: the shell builder. Reinhold Publishing Corporation; 1963.
[8] Veenendaal D, West M, Block P. History and overview of fabric formwork: using fabrics for concrete casting. Struct Concrete – J Fib 2011;12(3):164–77.
[9] Kersavage JA. Method for constructing a tensile-stress structure and resultant structures, patent us 3,927,496; 1975.
[10] Stepler R. Hypar structures, light, easy to build, cheap – and permanent. Pop Sci 1980;216(2):73,74–77,168.
[11] Knott A, Nez G. Latex concrete habitat. Canada: Trafford Publishing Company; 2005.
[12] Balding D. The experimental seismic testing of hypar shells. Fourth-year undergraduate project. Cambridge University; 2013.
[13] Carlton WS. Material behavior of latex-modified concrete in thin hyperbolic paraboloid shells. Master thesis. University of Oklahoma; 2013.
[14] Pronk A, Houtman R, Afink M. The reconstruction of the philips pavilion volume 1. In: Sources of architectural form, theory and practice. Kuwait City, Kuwait; 2007.
[15] Pronk A, Dominicus M. Philips-paviljoen; 2012.
[16] West M, Araya R. Fabric formwork for concrete structures and architecture. In: Krõplin B, Oñate E, editors. Proceedings of the international conference on textile composites and inflatable structures, structural membranes 2009. Barcelona; 2009.
[17] Cauberg N, Parmentier B, Vanneste M, Mollaert M. Fabric formwork for flexible, architectural concrete. In: Oehlers D, Griffith M, Seracino R, editors. Proceedings of the international symposium on fibre-reinforced polymer reinforcement for concrete structures, FRPRCS-9. Sydney, Australia; 2009.
[18] Cauberg N, Tysmans T, Adriaenssens S, Wastiels J, Mollaert M, Belkassem B. Shell elements of textile reinforced concrete using fabric formwork: a case study. Adv Struct Eng 2012;15(4):677–89.
[19] Ghaui B. My interests & thoughts as a part ii student; 2012. <http://ghaui.wordpress.com/tag/hyperbolic-paraboloid/>.

[20] Brennan J, Walker P, Pedreschi R, Ansell M. The potential of advanced textiles for fabric formwork. Construct Mater 2013;166(4):229–37.
[21] De Bolster E, Cuypers H, Van Itterbeek P, Wastiels J, De Wilde W. Use of hypar-shell structures with textile reinforced cement matrix composites in lightweight constructions. Compos Sci Technol 2009;69:1341–7.
[22] Mollaert M, Hebbelinck S. Adaptent: a generating system for cable net structures. In: Fifth international conference on space structures. Guildford, Surrey, UK; 2002.
[23] Waling J, Greszczuk L. Experiments with thin-shell structural models. In: Proceedings, annual meeting, American Concrete Institute, vol. 57; 1960. p. 413–31.
[24] Maddex D, Dow Alden B. Midwestern modern. Archetype Press; 2007.
[25] Waling J, Ziegler E, Kemmer H. Hy-par shell construction by offset wire method. In: Proceedings, world conference on shell structures. San Francisco, CA, US; 1962. p. 199–200. Washington, D.C., National Academy of Sciences-National Research Council Publication. p. 1187–453.
[26] Ortega NF, Robles SI. The design of hyperbolic paraboloids on the basis of their mechanical behaviour. Thin-Wall Struct 2003;41:769–84.
[27] Jadik T, Billington DP. Gabled hyperbolic paraboloid roofs without edge beams. J Struct Eng 1995;121:328–35.
[28] Tomás A, Martí P. Optimality of candela's concrete shells, a study of his posthumous design. J Int Assoc Shell Spatial Struct 2010;51(1):67–77.
[29] Guldentops L, Mollaert M, Adriaenssens, De Laet L, De Temmerman N. Textile formwork for concrete shells. In: Domingo A, Lazaro C, editors. Proceedings of the international association for shell and spatial structures (IASS) symposium 2009. Valencia; 2009. p. 1743–54.
[30] Tysmans T, Adriaenssens S, Wastiels J. Form finding methodology for force-modelled anticlastic shells in glass fibre textile reinforced cement composites. Eng Struct 2011;33:2603–11.
[31] Bletzinger KU, Wüchner R, Daoud F, Camprubí N. Computational methods for form finding and optimization of shells and membranes. Comput Methods Appl Mech Eng 2005;194:3438–52.
[32] Pugnale A, Sassone M. Morphogenesis and structural optimization of shell structures with the aid of a genetic algorithm. J Int Assoc Shell Spatial Struct 2007;48(3):161–6.
[33] Argyris J, Tenek L, Olofsson L. Tric: a simple but sophisticated 3-node triangular element based on 6 rigid body and 12 straining modes for fast computational simulations of arbitrary isotropic and laminated composite shells. Comput Methods Appl Mech Eng 1997;145:11–85.
[34] Argyris J, Papadrakakis M, Apostolopoulou C, Koutsourelakis S. The tric shell element: theoretical and numerical investigation. Comput Methods Appl Mech Eng 2000;182:217–45.
[35] Preisinger C. Karamba User Manual for Version 1.0.3; 2013.
[36] Linkwitz K, Schek H-J. Einige Bemerkungen zur Berechnung von vorgespannten Seilnetzkonstruktionen. Ing Arch 1971;40:145–58.
[37] Gründig L, Schek HJ. Analytical form finding and analysis of prestressed cable networks. In: International conference on tension roof structures. London, UK; 1974.
[38] Schek H-J. The force density method for form finding and computation of general networks. Comput Methods Appl Mech Eng 1974;3:115–34.
[39] Linkwitz K, Veenendaal D. Chapter 12: nonlinear force density method: constraints on force and geometry. In: Adriaenssens S, Block P, Veenendaal D, Williams C, editors. Shell Structures for Architecture. Routledge; 2014. p. 143–55.
[40] Linkwitz K. Formfinding by the "direct approach" and pertinent strategies for the conceptual design of prestressed and hanging structures. Int J Space Struct 1999;14(2):73–87.
[41] Barnes MR. Form finding and analysis of tension structures by dynamic relaxation. Int J Space Struct 1999;14(2):89–104.
[42] Máca P, Zatloukal J, Konvalinka P. Development of ultra high performance fiber reinforced concrete mixture. In: IEEE symposium on business, engineering and industrial applications; 2012.